Journal of Marine Research, 52, 397–426, 1994

Spring and winter water mass composition in the Brazil-Malvinas Confluence

by Keitapu Maamaatuaiahutapu[1], Véronique C. Garçon[1], Christine Provost[2], Mostefa Boulahdid[3] and Alejandro A. Bianchi[4]

ABSTRACT

Hydrographic data of the Confluence 1 cruise collected during austral spring (November 1988) have been analyzed to estimate relative mixing proportions of the various water masses of the Brazil-Malvinas Confluence region using a multiparameter analysis. Seven source water types (SWT) are identified in this region, and all are retained for the analysis: Thermocline Water (TW), Subantarctic Surface Water (SASW), Antarctic Intermediate Water (AAIW), Upper Circumpolar Deep Water (UCDW), North Atlantic Deep Water (NADW), Lower Circumpolar Deep Water (LCDW) and Weddell Sea Deep Water (WSDW). Tracers selected are temperature, salinity, dissolved oxygen and nutrients. Mixing proportions are quantified and plotted along five zonal sections at 35.4, 36.5, 37.9, 41 and 41.6S. The solution obtained during the springtime cruise is consistent with the wintertime (September 1989) data set (Maamaatuaiahutapu *et al.,* 1992): both show the large local recirculation of AAIW and the separation of NADW from the coast south of the thermocline front. However, noticeable changes in water mass mixing proportions can be detected between the winter of 1989 and the preceding spring. The seasonal change for the upper layers of TW and SASW is related to temporal and spatial fluctuations of the thermohaline front. The marked differences in SWT proportions between the two seasons occur at the same location for TW, SASW and AAIW; suggesting that the upper waters have a large impact on the AAIW movement. The deep waters undergo great spatial changes between the two cruises. The variation of the deep convergence position (revealed by the variation of spatial occupancy of the CDW and NADW) seems influenced by the movement of the thermocline front.

1. Introduction

In the western South Atlantic Ocean near the coast of Uruguay and Argentina, the warm subtropical waters of the poleward-flowing Brazil Current meet with the cold, less saline subantarctic waters of the northward-flowing Malvinas Current. The confluence of these currents forms a highly complex frontal structure. An overall

1. Unité Mixte de Recherche 39, Centre National de la Recherche Scientifique, Groupe de Recherche de Géodésie Spatiale, Toulouse, France.
2. Laboratoire d'Océanographie Dynamique et de Climatologie, Centre National de la Recherche Scientifique, Université Paris VI, Paris, France.
3. Institut des Sciences de la Mer et de l'Aménagement du Littoral, Algiers, Algeria.
4. Departamento de Oceanografía, Servicio de Hidrografía Naval, Buenos Aires, Argentina.

view of the complex Confluence dynamics is seen on maps of sea surface temperature (Legeckis and Gordon, 1982; Olson *et al.,* 1988; Provost *et al.,* 1992). The Brazil Current dominates the Malvinas Current and forces it in a cyclonic loop, before the merged current flows to the east at about 38S forming a broad subtropical convergence zone almost all the way across the South Atlantic Ocean (Peterson and Stramma, 1991). The meanders have a feedback effect: the warm water recirculates in a local anticyclonic cell and comes back to reinforce the Brazil Current (Peterson and Stramma, 1991). The local recirculation and mixing intensification at the frontal level play an important role not only in the ventilation of the thermocline but also in the transformation of water at every level of the water column. Gordon (1981) showed that in the poleward extension of the warm water, convective processes are important in ventilating the thermocline. These convective processes transfer salt and oxygen to mid-water depths and induce significant downward salt flux by salt-finger activity. A deep convergence also occurs between the circumpolar and the northern deep waters (Reid *et al.,* 1977). This encounter between waters of different origins induces a highly complex system, in which strong mixing and stirring processes develop (Georgi, 1981a). Furthermore, as a result of rapid cooling of the subtropical waters and intense photosynthetic utilization of CO_2 in the nutrient-rich Subantarctic waters, the Confluence zone is a strong sink for atmospheric CO_2 (Takahashi *et al.,* 1990). Thus, the Confluence region of the Brazil and Malvinas Currents represents a key region for understanding the circulation and heat transport of the South Atlantic as well as the global ocean-atmosphere CO_2 budget.

In 1988, an international group called "CONFLUENCE" was formed by Argentine, French and U.S. oceanographers (Confluence Group, 1990). Three oceanographic cruises were completed in three different seasons: austral spring, winter and summer One of the various objectives of the program is to gain a better understanding and a more accurate description of the circulation of water masses in the region.

As a first step in this direction, we perform a constrained least squares multiple tracer analysis of water mass composition in the Confluence region using Confluence 1 (spring cruise) and Confluence 2 data (winter cruise). Our analysis is based on the use of all available tracers to reconstruct a realistic picture of this region in terms of Source Water Types (SWT). This paper focuses on the analysis of the Confluence 1 data set and on the comparison with the Confluence 2 analysis presented in Maamaatuaiahutapu *et al.* (1992). The data acquisition is presented in Section 2. Section 3 recalls the complex water mass structure within the whole water column using Confluence 1 tracers as an illustration. The Least Squares Method is briefly described in Section 4. Section 5 shows the computed water mass composition for Confluence 1. The comparison with the Confluence 2 results are then discussed, followed by some concluding remarks.

2. Data

The Confluence data were collected aboard the R/V *Puerto Deseado* during the austral 1988 spring (November 2–26) for the Confluence 1 cruise and aboard the R/V *Oca Balda* during the 1989 winter (September 3–13) for the Confluence 2 cruise. The 35 and 28 conductivity-temperature-depth (CTD) casts performed during the Confluence 1 and 2 cruises were distributed along five and four east-west sections, respectively, across the continental slope (Fig. 1). Stations of the three northernmost sections are located approximately at the same positions during Confluence 1 and 2.

Seawater samples were collected from a 12-Niskin-bottle CTD rosette. All casts went close to the bottom. At each CTD station, a surface cast of up to four bottles was added to the unique cast in order to increase the vertical resolution in the upper ocean. Tracer analysis tasks were shared among the different participants of the Confluence program.

The CTD analysis and dissolved oxygen concentration measurements were carried out by the Oceanography Department of the Hydrographic Service of Argentina (Charo *et al.,* 1991).

Nutrient concentrations (silica, phosphate, nitrate and nitrite) were measured by the French scientists of Unité Mixte de Recherche (UMR) 39 and Laboratoire d'Océanographie Dynamique et de Climatologie (LODYC) in collaboration with the Algerian Institut des Sciences de la Mer et de l'Aménagement du Littoral (ISMAL). The automated analyses for nutrient determination were performed either immediately after sampling or after a few hours storage in a 4°C cold room. They were made using a Technicon Autoanalyzer AAII according to the techniques described by Boulahdid (1987). The instantaneous analytical reproducibility was established on deep water replicate samples. In the worst cases, nitrate, phosphate, and silicate measurements (expressed in the coefficient of variation) are obtained with a reproducibility of 0.9%, 0.8% and 1.5%, respectively (Garçon *et al.,* 1991). A comparison was carried out between Confluence 1 and 2, Geochemical Ocean Sections Study (GEOSECS), and South Atlantic Ventilation Experiment (SAVE) leg 5 data on deep waters to detect the presence of systematic errors. When necessary, the appropriate relative corrections were applied to the Confluence 1 and 2 data sets (Garçon *et al.,* 1991).

3. Core layers

The tracer charts are generally used to distinguish the different core layers and to follow the different paths of these core layers within the ocean (see for example Reid, 1989). Seven main core layers were identified in the southwestern Atlantic Ocean around the Confluence region (Reid *et al.,* 1977; Greengrove, 1986; Peterson, 1992). Extrema in tracer profiles are associated with these seven core layers. Two

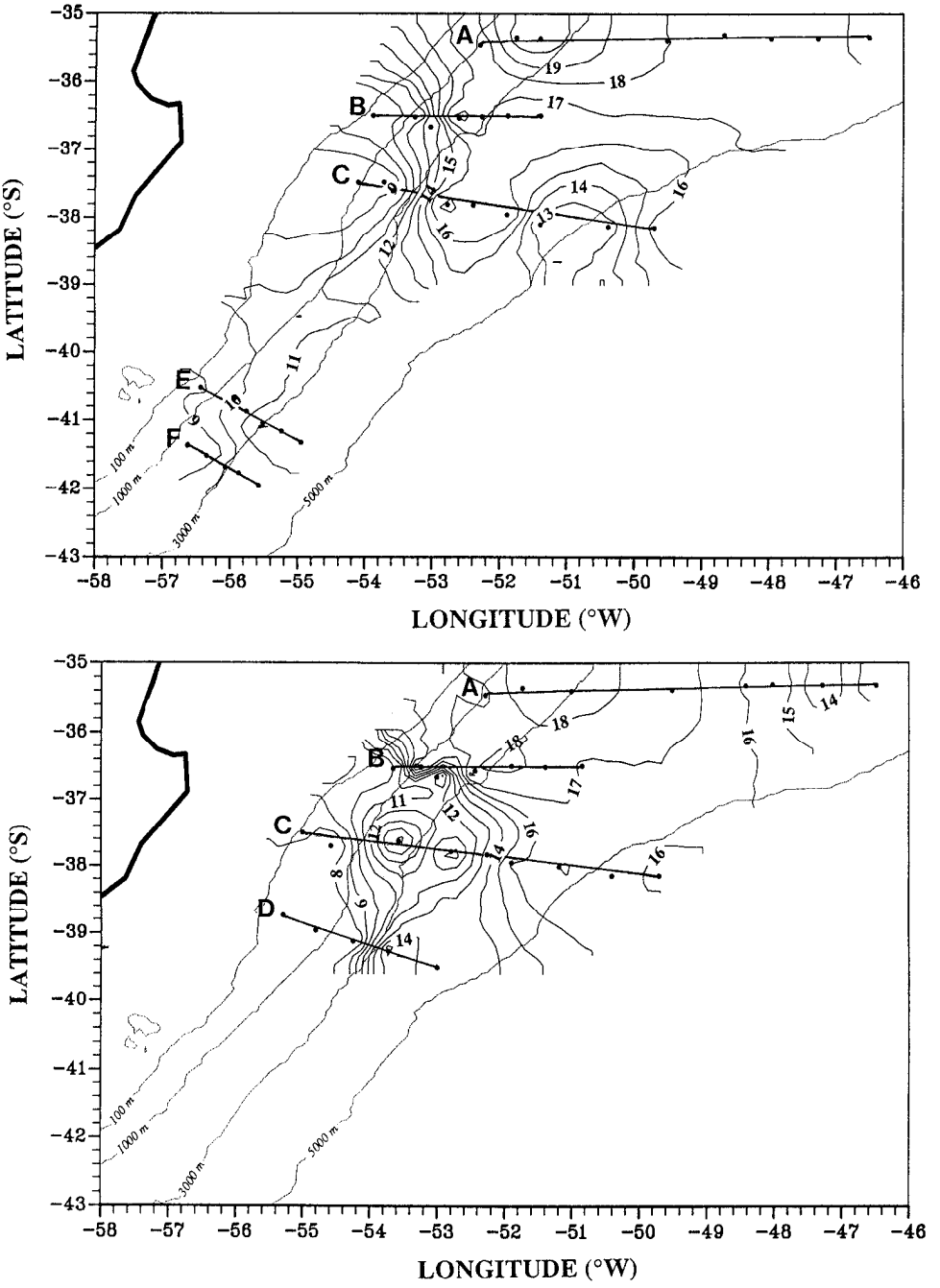

Figure 1. (a) Location of CTD stations of the oceanographic cruise Confluence 1 along five east-west sections (dots along sections A, B, C, E, F; November 1988). The sea surface temperature contours are drawn with a 1°C interval. The 100-, 1000-, 3000-, and 5000-m isobaths are shown; (b) Location of CTD stations of the oceanographic cruise Confluence 2 along four east-west sections (dots along sections A, B, C, D; September 1989). The sea surface temperature contours are drawn with a 1°C interval. The 100-, 1000-, 3000-, and 5000-m isobaths are shown.

sections (sections A and E, Fig. 1) were chosen from the Confluence 1 data set to characterize the various core-layers in the Confluence region (Figs. 2 and 3). Section A is the northernmost Confluence section; it is used to illustrate poleward water flow. The southern water masses are best visualized in section E. A compilation of the data sets of the two cruises is available in Charo *et al.* (1991) and Garçon *et al.* (1991). Here we succinctly present the main characteristics of each core layer.

The upper level is marked by a strong thermohaline front due to the encounter of two major ocean currents: the Brazil Current (BC), which transports warm and salty water (the Thermocline Water, TW) southward and the Malvinas Current (MC) which transports colder and fresher water (the Subantarctic Surface Water, SASW) northward. The BC leaves the shelf in the Confluence area and flows southward for some distance together with the return flow of the MC. The TW enters the Confluence area from the north and is best observed in section A (Fig. 2). It is the warmest and saltiest water with temperature higher than 16°C and salinity up to 36.00 psu (Fig. 2a). The lowest nutrient (nitrate, phosphate, silica) concentrations are also attributed to the TW (Figures 2b–2c). In section E, low temperature and salinity values are observed (Fig. 3a). These values are due to Subantarctic Surface Water (SASW) intrusion in the Confluence area. The SASW is richer in oxygen and nutrient contents than the TW (Figs. 2–3). The SASW is compressed onto the shelf as it moves northward (Maamaatuaiahutapu *et al.,* 1992). We found fresh water on the western part of section E (Fig. 3a). This slope water (Gordon, 1981) forms a new mixture with SASW, carried by the Malvinas current into the Confluence area. This mixture will be identified as our SASW component, as discussed later. SASW has a salinity of around 34.10 psu and forms a 400 m deep layer at section E.

A homogeneous core of salinity minimum (around 34.30 psu) beneath the TW at about 1000 m in section A (Fig. 2a) marks the Antarctic Intermediate Water (AAIW) (see Reid *et al.,* 1977). The same salinity value is found at shallower depth (around 600 m) farther south (Fig. 3a), but with a less distinct core than at the northern section. AAIW coincides with a local oxygen maximum (Fig. 2b).

In the Southwestern Atlantic Ocean, two major deep core layers have been identified: the Circumpolar Deep Water (CDW) and the North Atlantic Deep Water (NADW) (Reid *et al.,* 1977; Peterson and Whitworth, 1989). The CDW flows northward along the continental margin (Reid *et al.,* 1977; Peterson and Whitworth, 1989) as a single core south of the Confluence region. North of the Confluence region, it separates into two branches: the upper CDW (UCDW) above the NADW and the lower CDW (LCDW) below the NADW. The Confluence region is a transition zone where the NADW, spreading southward in an anticyclonic gyre, meets the CDW on the western boundary (Gordon, 1989; Maamaatuaiahutapu *et al.,* 1992). The sections A and E describe how the encounter between NADW and CDW occurs during the Confluence 1 cruise.

The oxygen minimum core discussed by Reid *et al.* (1977) corresponds to the

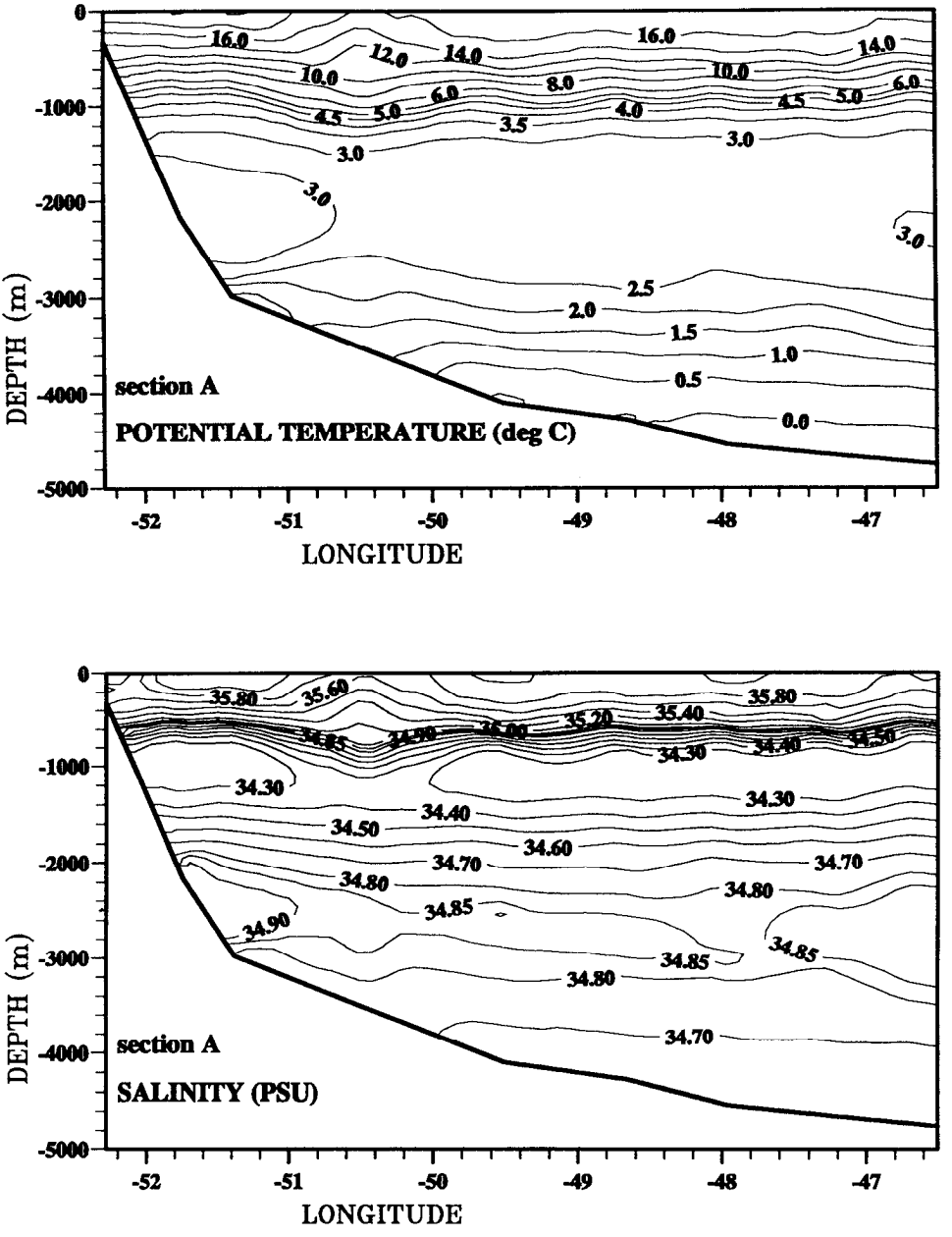

Figure 2. (a) Potential temperature (°C) and Salinity (psu) along the Confluence 1 section A. The section is limited on the west and on the east by a CTD station; (b) Oxygen (ml/l) and Nitrate (μmol/kg) along the Confluence 1 section A. The section is limited on the west and on the east by a CTD station. The samples are located by dots; (c) Phosphate (μmol/kg) and Silicate (μmol/kg) along the Confluence 1 section A. The section is limited on the west and on the east by a CTD station. The samples are located by dots.

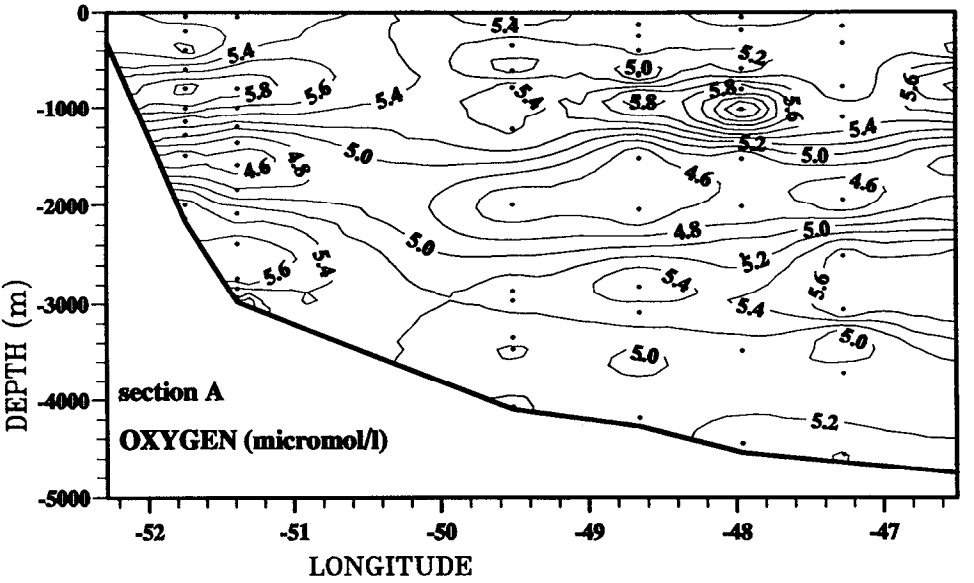

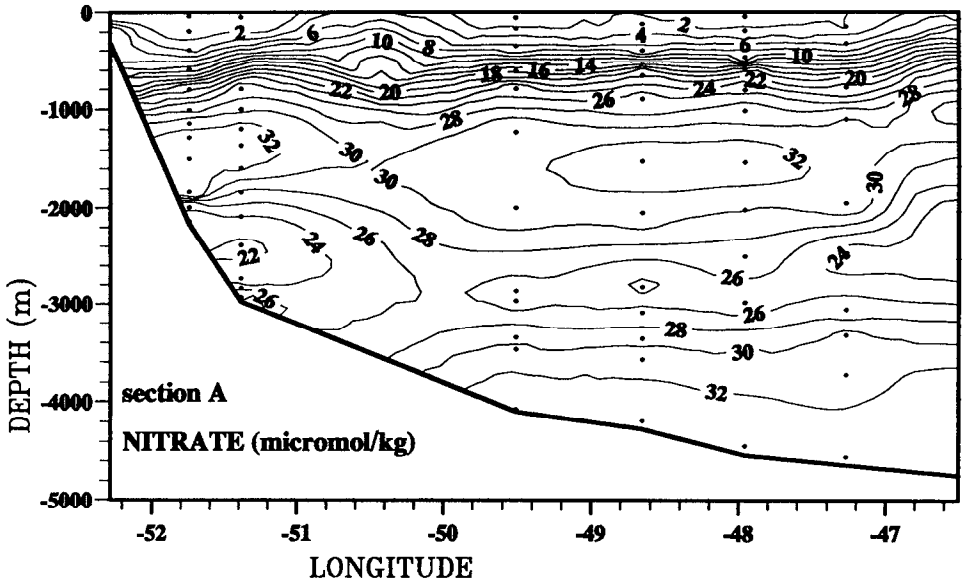

Figure 2. (Continued)

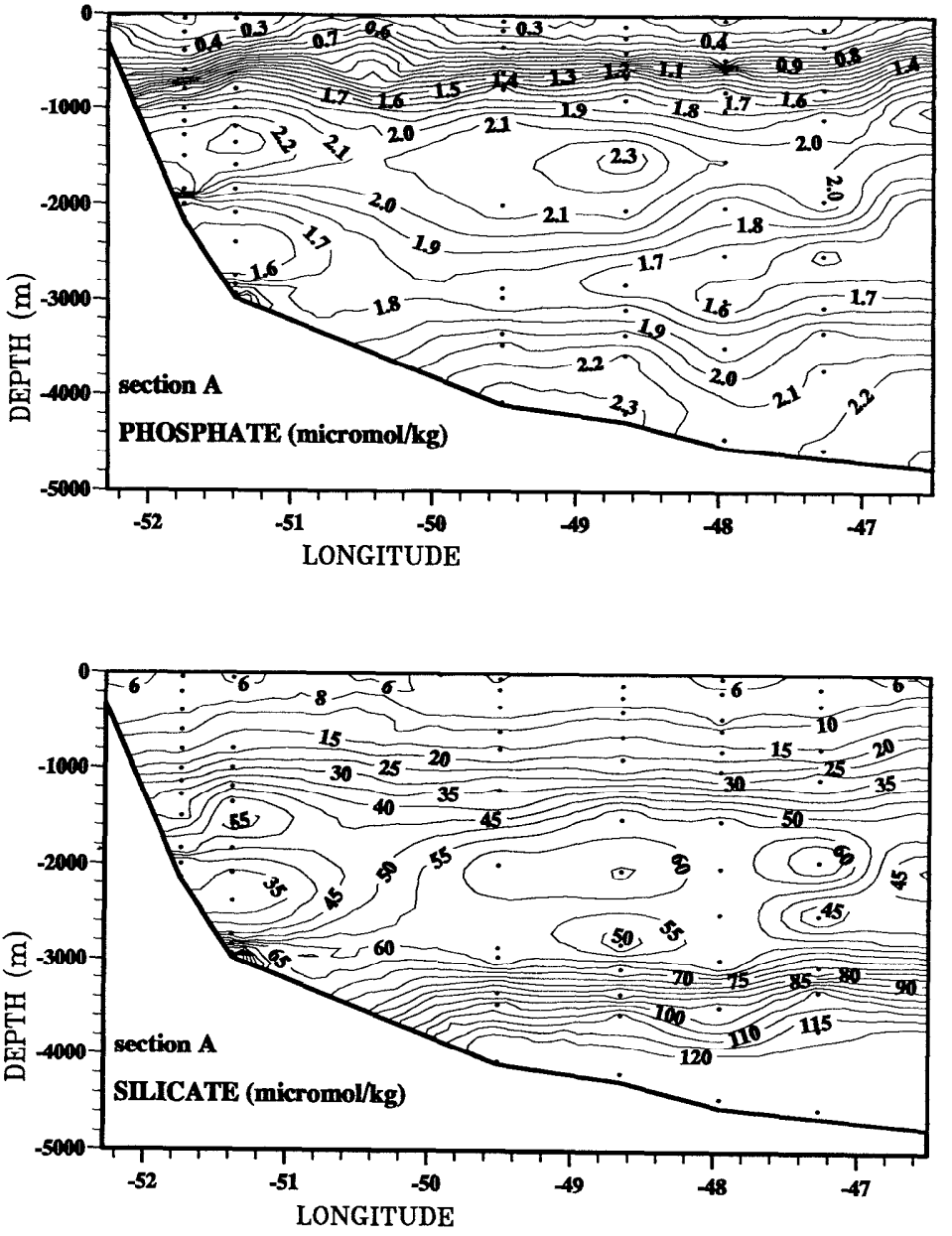

Figure 2. (Continued)

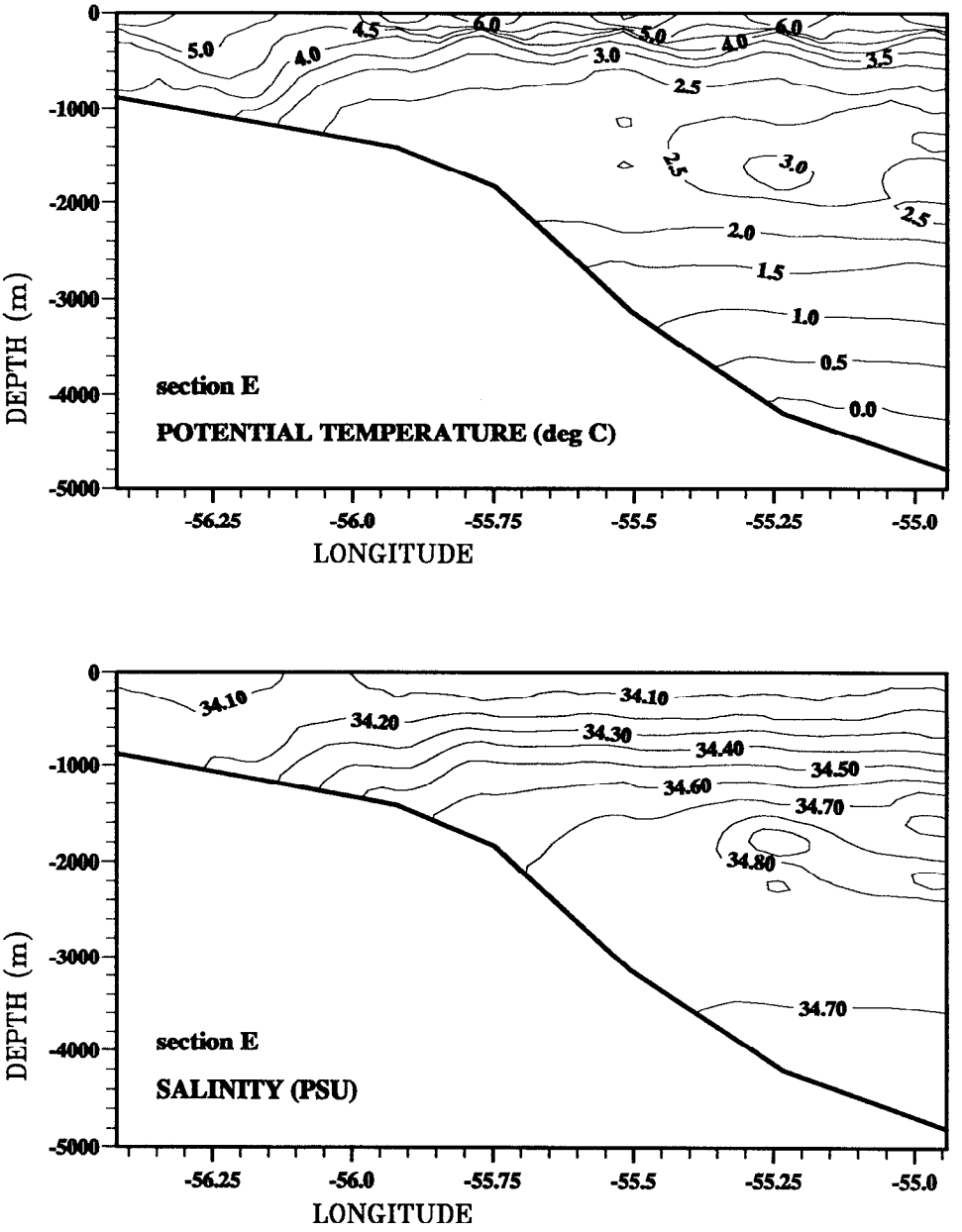

Figure 3. (a) Potential Temperature (°C) and Salinity (psu) along the Confluence 1 section E. The section is limited on the west and on the east by a CTD station; (b) Oxygen (ml/l) and Nitrate (μmol/kg) along the Confluence 1 section E. The section is limited on the west and on the east by a CTD station. The samples are located by dots; (c) Phosphate (μmol/kg) and Silicate (μmol/kg) along the Confluence 1 section E. The section is limited on the west and on the east by a CTD station. The samples are located by dots.

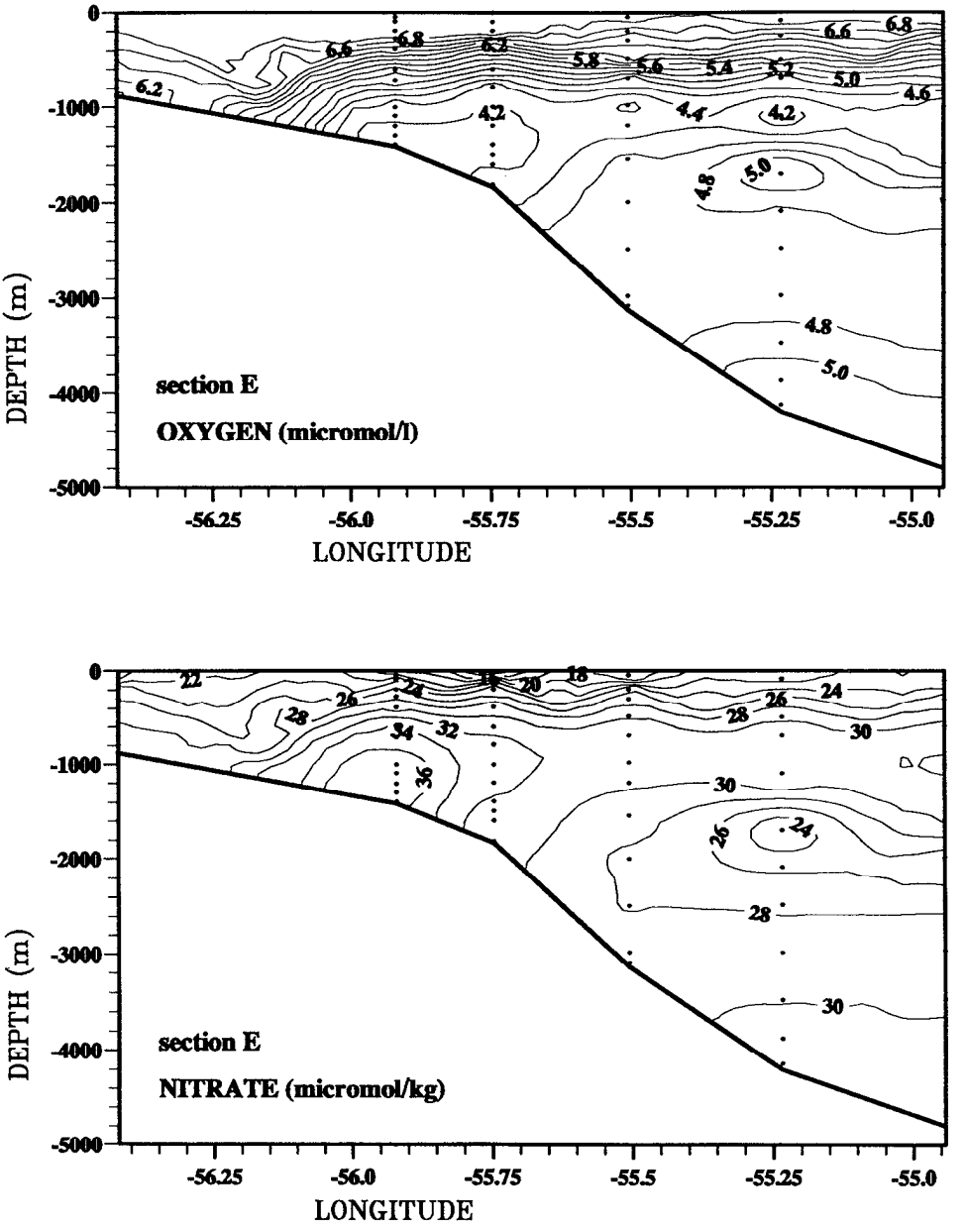

Figure 3. (Continued)

CDW. At Confluence 1 section A, between 1200 m and 2000 m, a minimum oxygen core layer extends from west to east (Fig. 2b). The UCDW is associated with a relative maximum in phosphate and nitrate (Figs. 2b, 2c). At the southern section E (Fig. 3), the same characteristics are located at a depth range of 800 m to 1400 m.

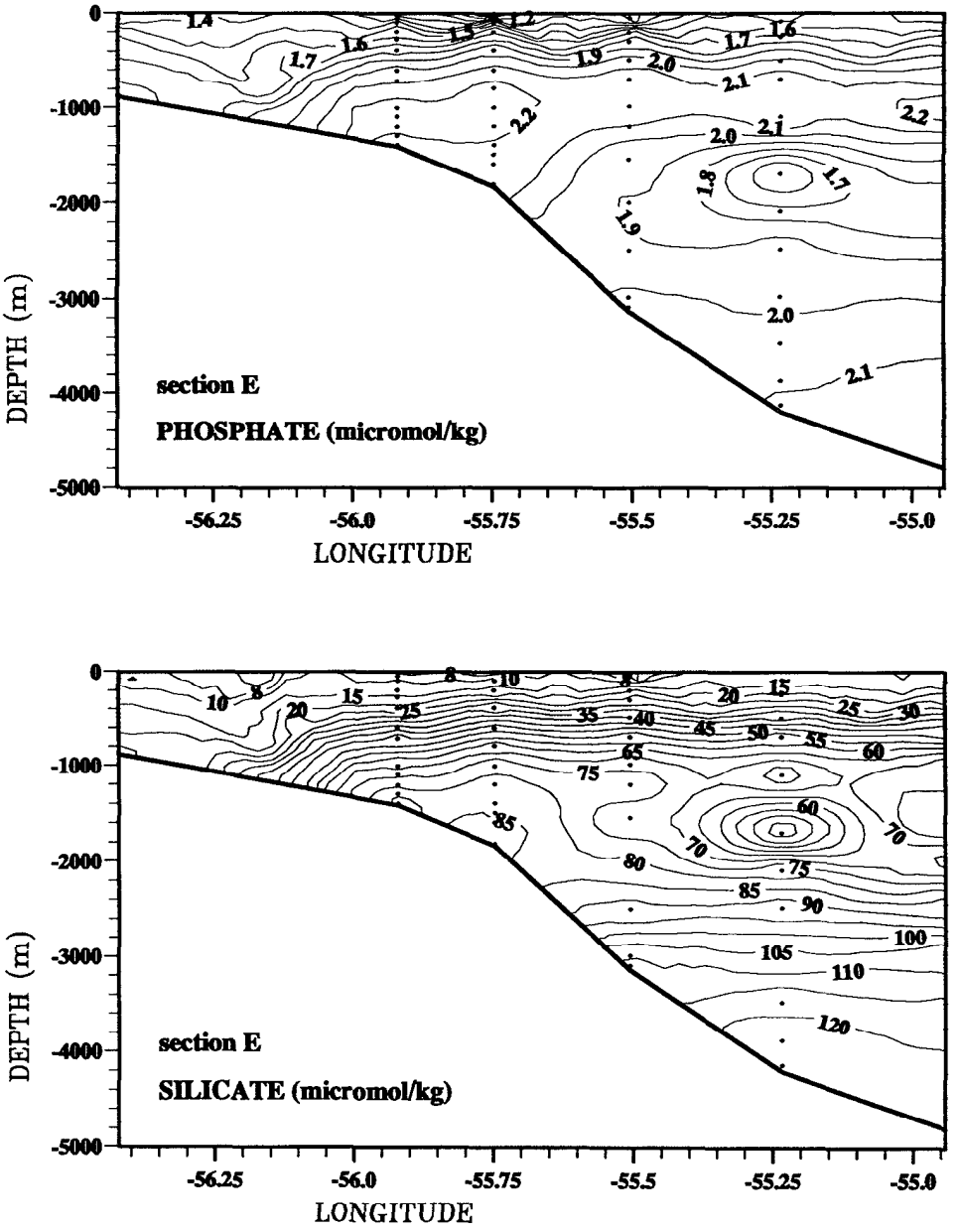

Figure 3. (Continued)

The main core of NADW is distinguished between 2000–2800 m by high values in salinity (34.85 psu) and slightly higher temperature than UCDW (Fig. 2a). At the same depth level, relatively higher oxygen and lower nutrient concentrations are observed (Fig. 2b, 2c). The NADW appears within two cores at section A (Fig. 2),

one compressed on the continental slope and the other further east. The NADW core around 2000 m is reduced on section E (Figure 3) and only a minor contribution is found in the east.

At section A, the second oxygen minimum corresponding to the LCDW (see Reid *et al.,* 1977) has no clear signature like the UCDW oxygen minimum (Fig. 2b). On the southern section E, an oxygen minimum locates the LCDW.

The abyssal layer, the Weddell Sea Deep Water (WSDW) is generally considered the coldest water with temperature below 0°C (Georgi, 1981b) (Figs. 2 and 3); this water spreads northward. WSDW is characterized by relatively high concentration of nutrients.

In Figures 2 and 3, we see that tracer extrema illustrate each SWT for the small investigated area. However, the description of water masses based on tracer patterns remains qualitative and difficult to perform. A more quantitative technique is proposed here with the constrained least-squares method where every piece of information brought out by the different tracers is considered.

4. Multiparameter analysis

The method of multiparameter analysis is presented in Maamaatuaiahutapu *et al.* (1992) and a brief résumé is made here. The purpose is to find the mixture of SWT that best describes the composition of a given water sample. The efficiency of such a method in a frontal area compared with classical *T-S* analyses is discussed in Tomczak (1981) and Mackas *et al.* (1987). The computational problem is to search for an n-vector $\mathbf{x}$ containing the n-SWT proportions which minimizes the weighted sum of squares of deviation D^2 between p-measured data (vector $\mathbf{b}$) and p-estimates of model parameters (vector $\mathbf{Ax}$),

$$D^2 = (\mathbf{Ax} - \mathbf{b})^T W^{-1}(\mathbf{Ax} - \mathbf{b}).$$

A and W are two matrices which will be defined below. Superscripts (T) and (-1) denote the vector transpose and the matrix inverse, respectively. It is a matricial calculation where mass conservation is applied and each component of the solution vector $\mathbf{x}$ is required to be positive. The problem is solved using a non-negative least squares algorithm (Lawson and Hanson, 1974; Menke, 1989). The application of this multiparameter analysis based on a least-squares method requires the definition of the two matrices, A and W.

Matrix A contains the characteristics of the SWT evolving around the Confluence region. The seven SWT listed previously (TW, SASW, AAIW, UCDW, NADW, LCDW, WSDW) are all included in our analysis. The p-tracers available are temperature, salinity, dissolved oxygen and nutrients. To perform a comparison between the data measured during Confluence 1 and Confluence 2, we decided to keep the matrix A defined by Maamaatuaiahutapu *et al.* (1992) (Table 1).

The matrix W is a variance-covariance matrix tabulating the observed statistical

Table 1. Tracer characteristics of primary source water types compiled from historical data and estimated standard deviation for each tracer. The weighting matrix is derived by inverting the matrix $W = \sigma^2 I$, where I is the identity matrix (Maamaatuaiahutapu *et al.*, 1992).

	MATRIX A							
Tracers	TW (×1)	SASW (×2)	AAIW (×3)	UCDW (×4)	NADW (×5)	LCDW (×6)	WSDW (×7)	MATRIX W: σ
T, °C	16.0	5.0	4.0	2.5	3.00	1.50	−0.20	0.25
S, psu	35.8	34.1	34.2	34.6	34.92	34.76	34.68	0.07
NO_3^-, μm/kg	6.0	17.0	26.5	29.0	23.50	29.00	31.00	1.12
PO_4^{3-}, μm/kg	0.5	1.9	1.9	2.2	1.70	1.80	2.20	0.15
SiO_2, μm/kg	5.0	10.0	20.0	70.0	30.00	102.00	121.00	1.50
O_2, ml/l	5.4	6.0	5.6	4.6	5.60	4.75	5.25	0.13
$\Sigma_i x_i = 1$	1.0	1.0	1.0	1.0	1.00	1.00	1.00	0.01

variability in the samples and in the SWT. It is of great importance as it assigns a weight to each tracer. High weights (low values in W) are given to tracers measured with the greatest relative accuracy. To accomplish a meaningful comparison between the Confluence 1 and 2 cruises, we take the same diagonal weighting matrix W as in Maamaatuaiahutapu *et al.* (1992) (Table 1).

The sensitivity and robustness of the results are analyzed using perturbation experiments. One hundred random perturbations are made on each SWT of the matrix A. Thus, one hundred solutions are obtained with one hundred different matrices A. The SWT characteristics fluctuate with values bounded by standard deviations specified in the matrix W around values specified in the matrix A. The solution presented in the next paragraph for the Confluence 1 cruise is the mean of one hundred solutions. The perturbation experiments show how stable the problem is (see Lawson and Hanson, 1974). The sensitivity of each SWT in each sample can be expressed by a standard deviation value. Table 2 indicates (for the two cruises and

Table 2. Percentages of water samples, for each Source Water Type, with a standard deviation value less than 5, 10, 15% for both Confluence 1 and Confluence 2 cruises. The TW values are not reported, the standard deviation being always lower than the strictest criteria (5%). The Mean values represent the average of the percentages of water samples, for a given criterion, of all seven SWT.

Cruise	Criterion	SASW	AAIW	UCDW	NADW	LCDW	WSDW	Mean
Confluence 1	5%	91.8	84.5	97.0	79.3	85.3	85.6	89.0
	10%	99.7	94.3	99.7	89.1	92.9	95.1	95.8
	15%	100	99.5	100	96.5	97.3	99.5	98.9
Confluence 2	5%	86.7	88.6	97.5	85.0	89.7	89.2	90.9
	10%	99.7	94.0	99.7	89.0	96.0	97.0	96.6
	15%	100	98.8	100	96.0	98.6	100	99.1

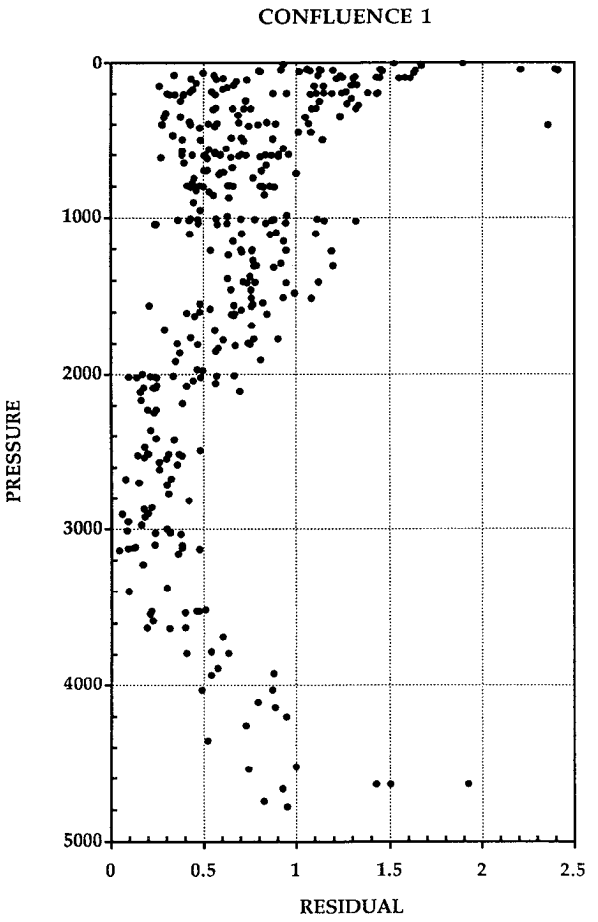

Figure 4. Residuals versus pressure for all Confluence 1 samples.

for each SWT) the percentage of analyzed water samples with a standard deviation value smaller than 5, 10 and 15%. Based on these criteria, the average percentage of samples (taking into account all the SWT of the two cruises) is 90% for the 5% criteria, 96% for the 10% criteria, and 99% for the 15% criteria.

The residuals (defined as $D^2/(p + 1)$) are high at certain locations (Fig. 4). We find samples with a poor fit near the sea surface. Two reasons may be put forward for this: the local nonconservation of tracers and the poor characterization of water masses near the surface. Indeed, biological activity, intense in the euphotic zone, acts as a sink for nutrients and as a source for dissolved O_2. Gas exchange at the air-sea interface controls the O_2 evolution. We therefore overestimate nutrients and underestimate O_2 in the upper ocean in our description. The surface waters also have their *T-S* properties affected by direct warming or cooling from the atmosphere and by precipitation or evaporation. The water samples are not always perfectly represented

by the water masses described in Table 1. Other SWT must contribute to the melting pot. Our SASW component is in fact a mixture of slope water, river plume water from Río de la Plata, and real SASW advected by the Malvinas Current (Gordon, 1981). It is difficult to give tracer characteristics to the TW and SASW because tracers have such a broad range of variation (e.g., for TW, temperature can vary from 10°C to 18°C). Here, the TW includes the warmest and/or saltiest waters; the SASW contains all the waters with low salinity, that are warmer and more oxygenated than AAIW. Evidence of local nonconservation of tracers around 1500 m is observed (Fig. 4). This is mainly due to oxygen consumption and nutrient release. Similarly, scattered residuals within bottom waters (4000–5000 m) are essentially the result of poor prediction of silicate values.

5. Water mass concentrations for the Confluence 1 cruise

Here we present and discuss the concentrations of each SWT analyzed from the Confluence 1 cruise (Fig. 5). They are comparable to the Confluence 2 results as detailed in Maamaatuaiahutapu *et al.* (1992).

The upper layer samples are shared among the warm-salty TW and the cold-fresh SASW. The upper level of the study area is globally divided into two parts, the northern part occupied by the TW (Fig. 5a) and the southern part occupied by the SASW (Fig. 5b). The TW has high concentrations (above 90%) on the northernmost section A (35.4S) from the surface to a depth of 500 m. With the Brazil Current, the TW moves southward and leaves the continental shelf. Its presence on section B (36.5S) is restricted east of 53W, whereas on section C (37.9S) the TW at shallower depth contributes 90% of the water sample between 52–53W and at 50W (Fig. 5a). The TW completely vanishes on the two southernmost sections E (41S) and F (41.6S). In spite of the absence of the TW on the southern sections, little SASW contributes to the water samples (Fig. 5b). Only a thin SASW surface layer (100 m–150 m) is observed between 55.2–56W and 56–56.5W on sections E (41S) and F (41.6S), respectively. In the north on sections B and C, the analysis suggests that this water is compressed onto the shelf, west of 53W.

In the Confluence region, the Antarctic Intermediate Water dominates the depth range of 400–1100 m (Fig. 5c). Its percentage is higher on the three northern sections than on the southern ones. A homogeneous 70% core extends all along these three northern sections. The AAIW is found at shallower depths within the Malvinas Current than underneath the Brazil Current and it does not form a thick distinct layer on the two southern sections E and F.

NADW and CDW have very different tracer concentrations and the convergence creates large variations in the tracer fields. Very few samples in our mixing analysis have more than 90% proportion of either northern or circumpolar deep waters (Fig. 5d,e,f). On the two sections E and F, the CDW forms a single core extending from west to east in the depth range of 1000 to 4000 m. In its northward flow, the

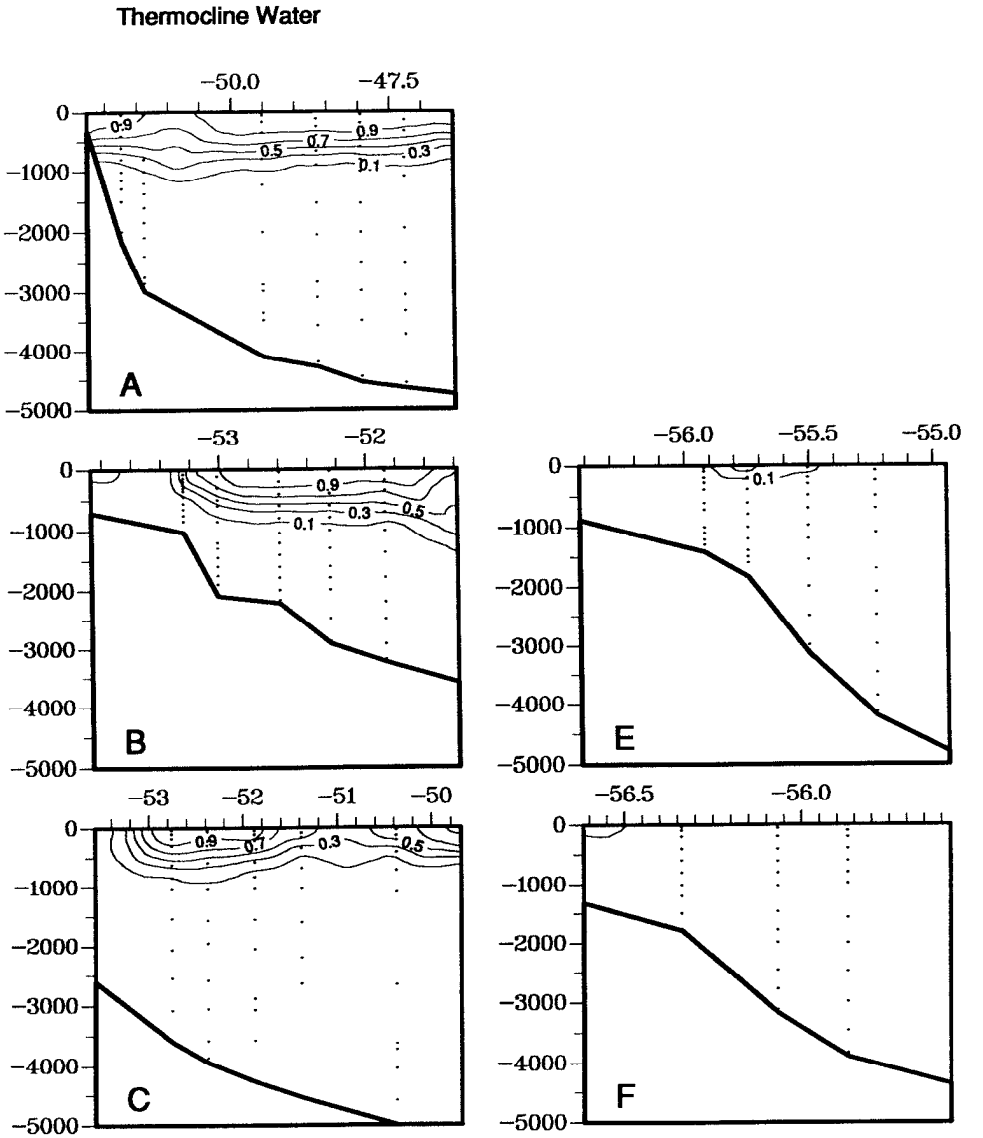

Figure 5. Source composition solution along the five Confluence 1 sections (A, B, C, E, F) showing concentration of the seven source water types: (a) Thermocline Water (TW), (b) Subantarctic Surface Water (SASW), (c) Antarctic Intermediate Water (AAIW), (d) Upper Circumpolar Deep Water (UCDW), (e) North Atlantic Deep Water (NADW), (f) Lower Circumpolar Deep Water (LCDW) and (g) Weddell Sea Deep Water (WSDW). Sample locations are indicated by dots. Isoline interval is 0.2. Each section is limited on the west and on the east by a CTD station.

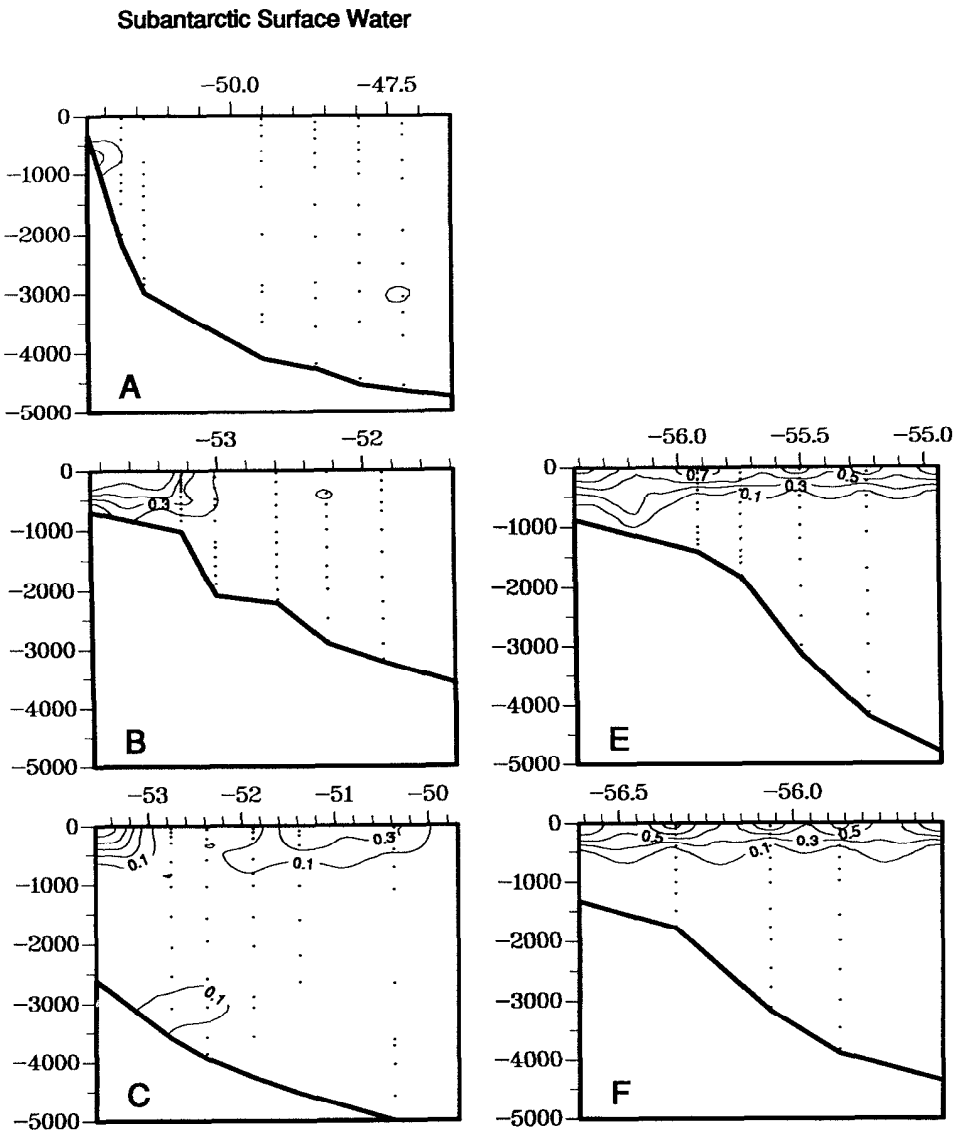

Figure 5. (Continued)

CDW is split into the UCDW and the LCDW by the poleward NADW flow. Our solution shows that a large part of the CDW feeds the UCDW while a relatively small quantity of LCDW is present in the investigated area (Fig. 5d,f). The UCDW forms a homogenous 70% layer at 41S (section E) and 41.6S (section F). Farther north, the UCDW 70% core is separated into isolated patches. One of them flows northward along the slope (sections C and B). However, on section A, it is located more to the

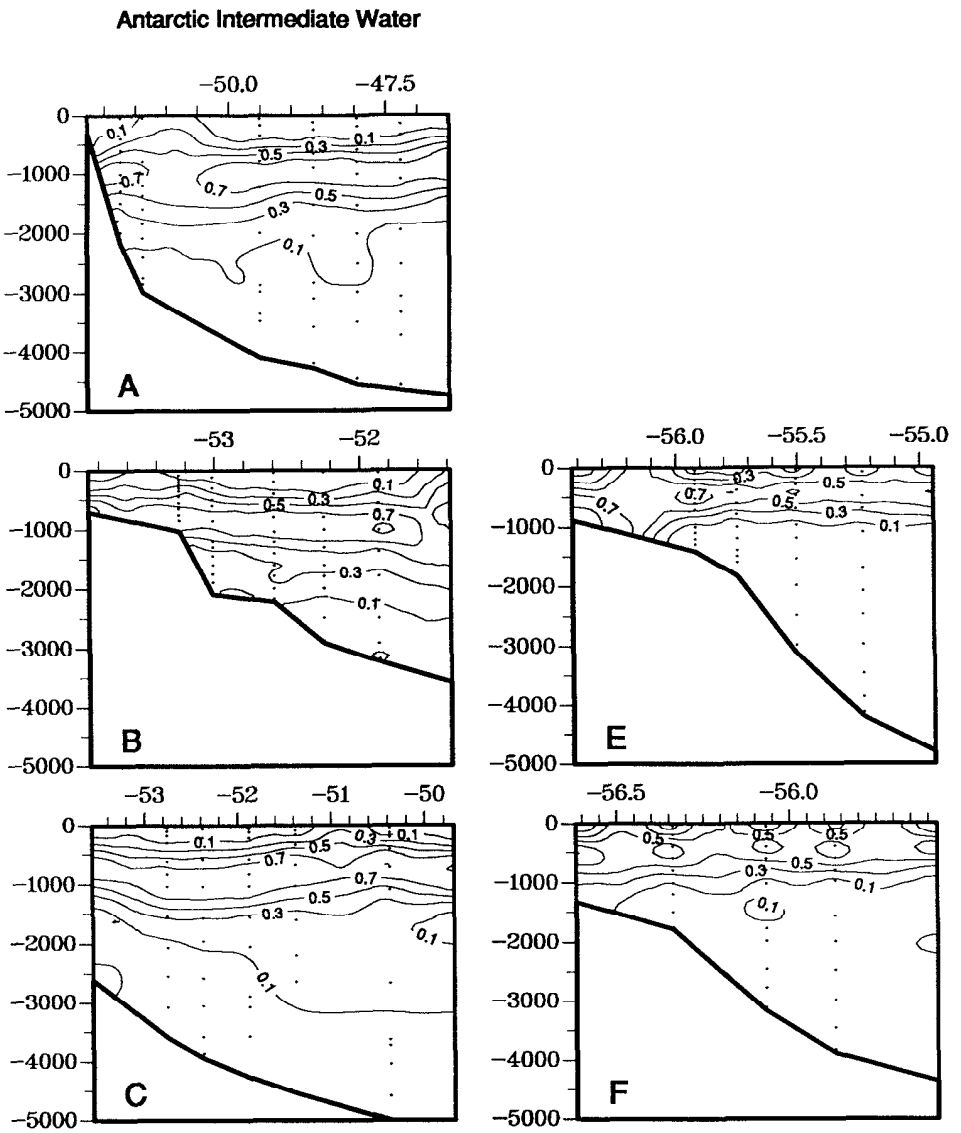

Figure 5. (Continued)

east, between 47.5W and 50W. The NADW progresses southward in close proximity to the continental slope (sections A, B on Fig. 5e). Values of up to 88% are found at 35.4S (section A) and 36.5S (section B). Along its trip, the NADW is shifted to the east by the CDW and leaves the slope. On section C, the 50% NADW core is detached from the western boundary. On section E, a remnant of NADW is observed at the 1500 m level. On the southernmost section F, no more NADW is present.

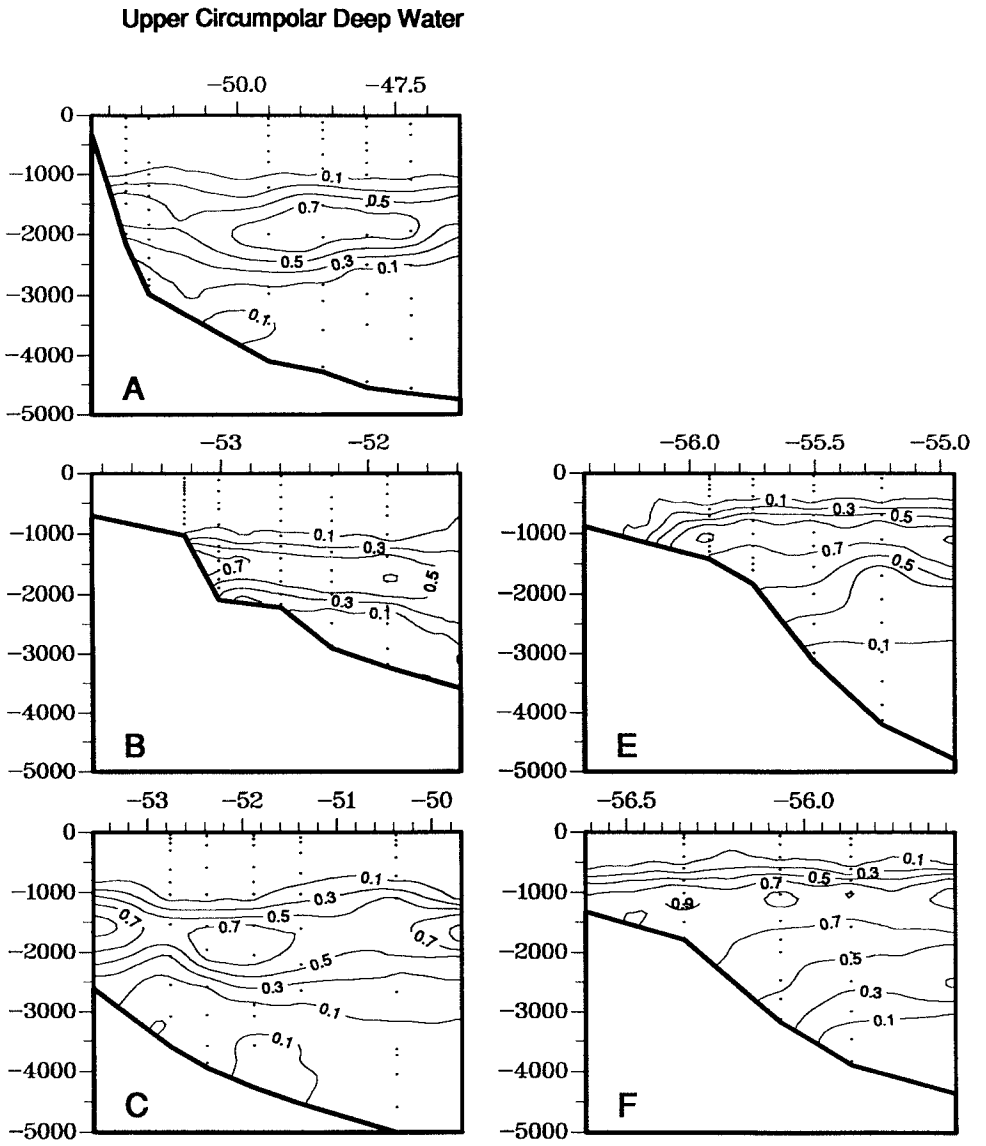

Figure 5. (Continued)

The Lower Circumpolar Deep Water, like the UCDW, has the highest contributions south of 40S (55% to 78% at a depth of 3000 m, Fig. 5f). Its contribution decreases rapidly toward the north. The poor contribution of the LCDW to the water sample is consistent with the oxygen field described in Section 3 (Figs. 2b and 3b). The LCDW northward flow is forced back by or moves eastward with the NADW.

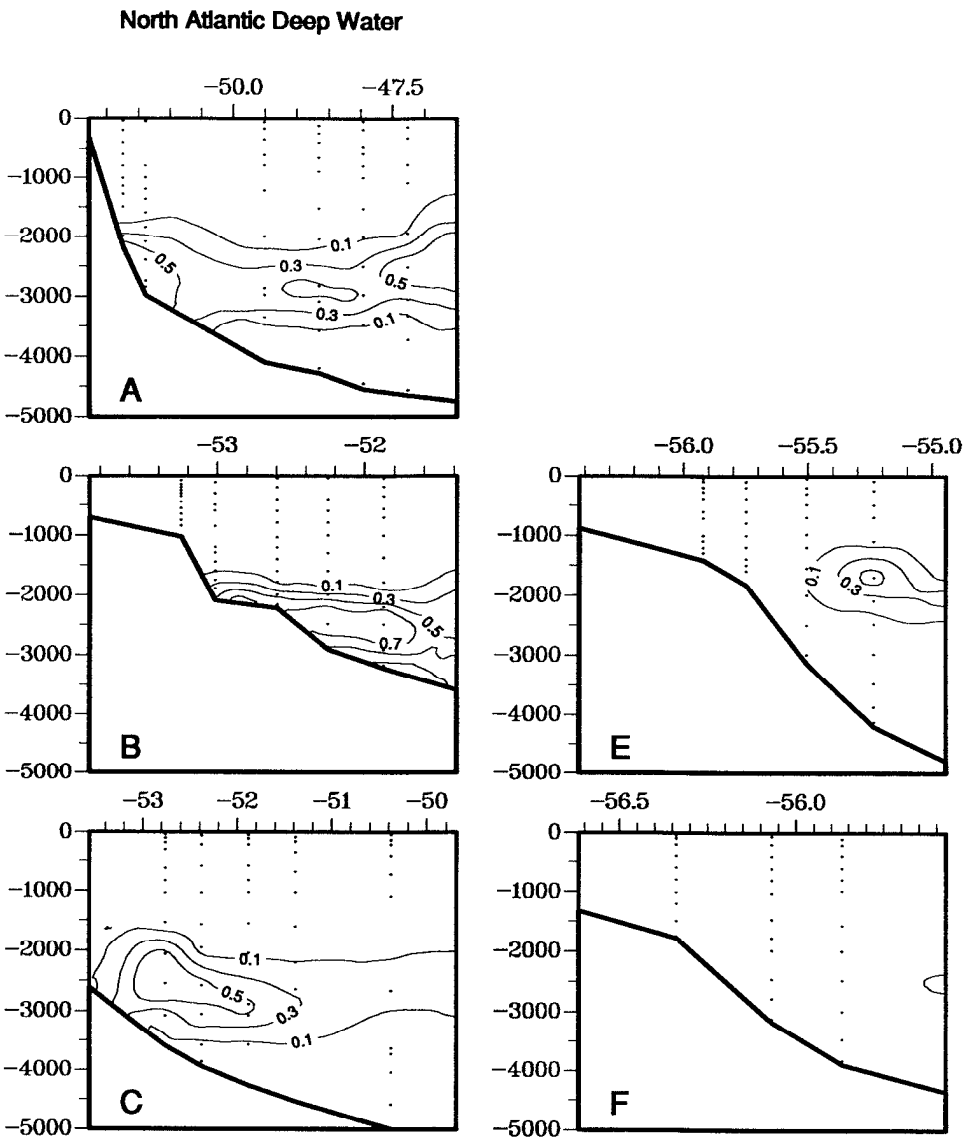

Figure 5. (Continued)

The Weddell Sea Deep Water is well marked (higher than 90%) on the bottom except on section B, where topography does not exceed 3500 m (Fig. 5g).

6. Discussion

The hydrographic data of the Confluence 1 and 2 cruises, collected during austral spring and winter, respectively, have been analyzed to estimate the relative mixing

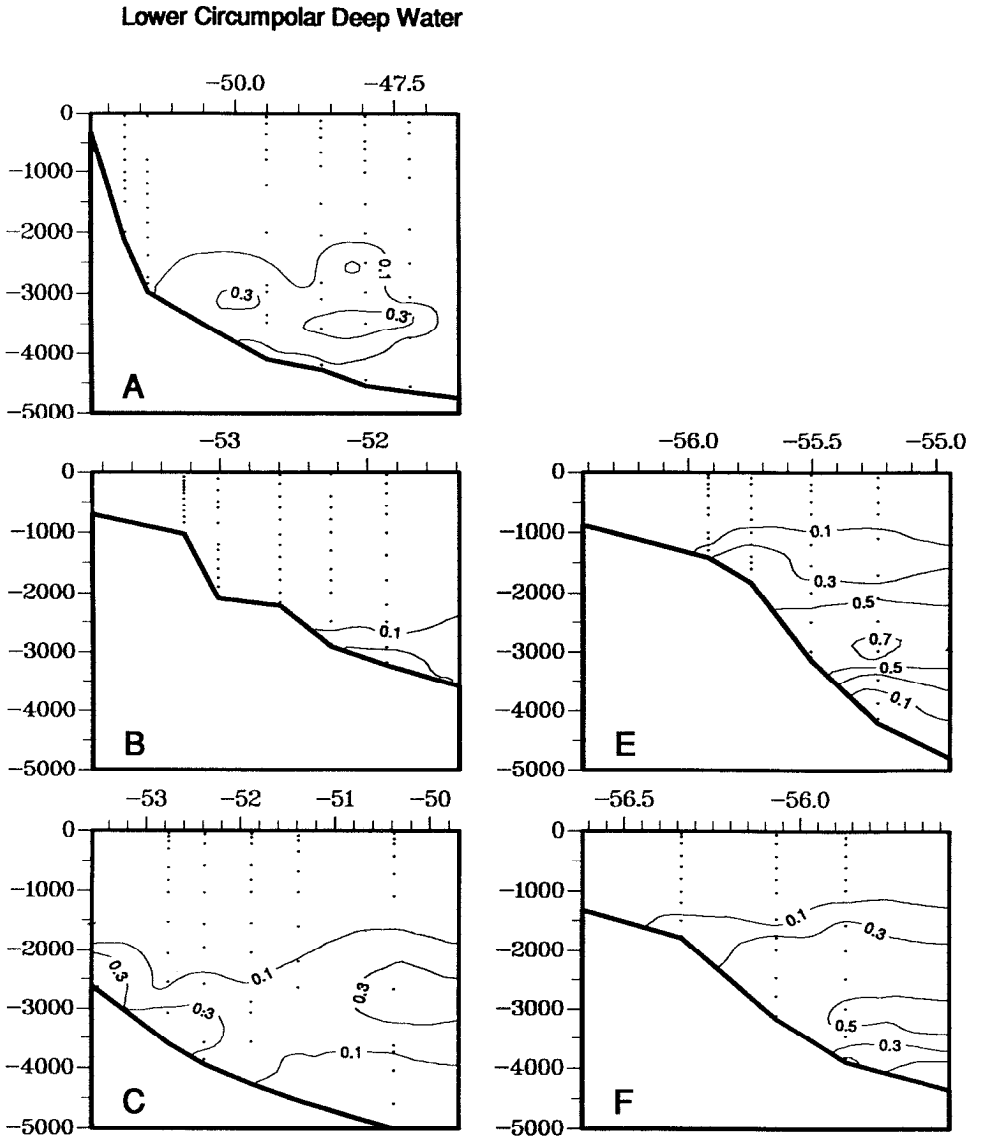

Figure 5. (Continued)

proportion of the water masses of the Brazil-Malvinas confluence region by means of a multi-parametric analysis with an inverse methodology (Section 5 of this paper for Confluence 1; in Maamaatuaiahutapu *et al.* (1992) for Confluence 2). The low vertical sampling resolution due to bottle data may have been a problem. Comparison with a SAVE section (Maamaatuiahutapu *et al.*, 1992), for which 36 water samples are obtained vertically, shows that the vertical resolution of the Confluence

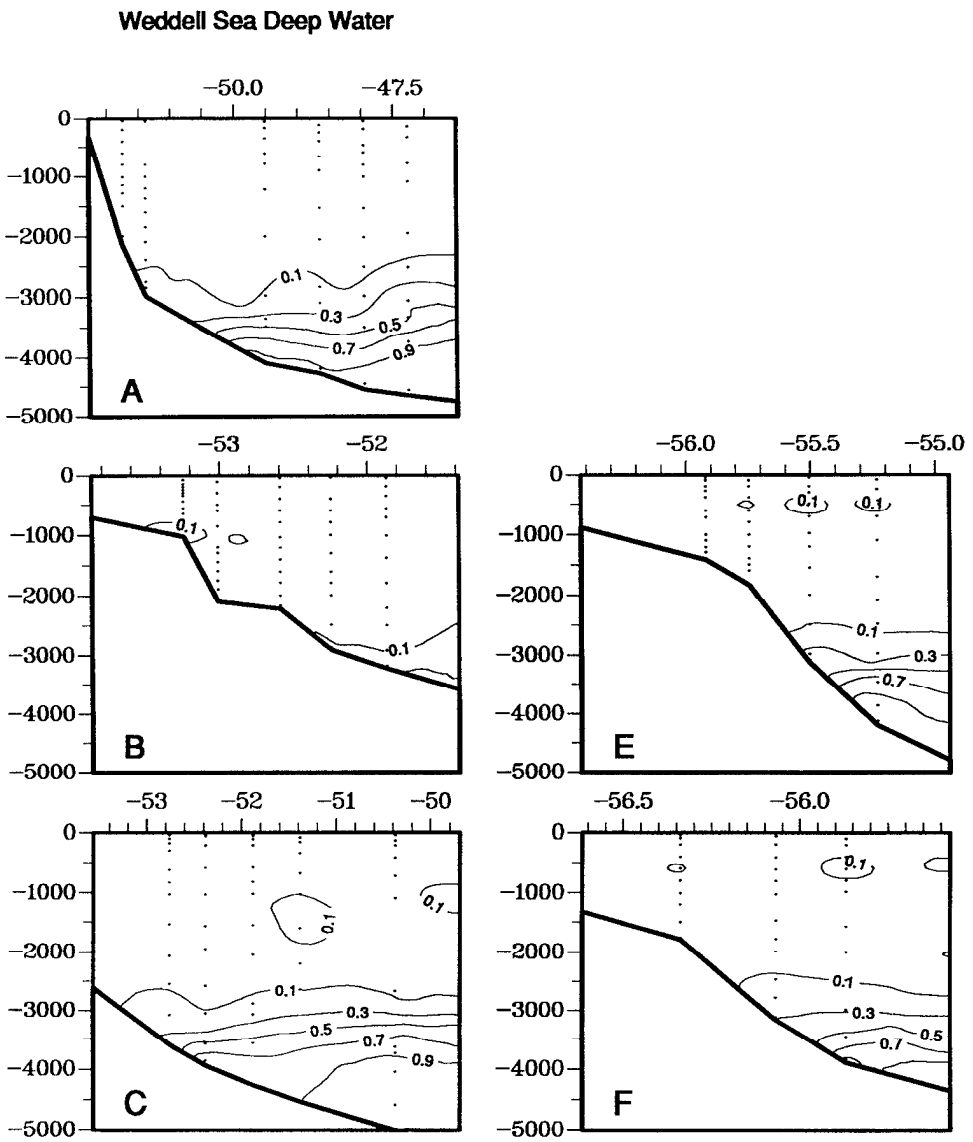

Figure 5. (Continued)

1 and 2, stations for which the maximum number of water samples can reach 16, is quite good to describe the different core layers.

The same general picture of the water mass circulation is obtained with the two data sets. As pointed out by Gordon (1989), the separation point of the southward flowing western boundary current occurs at different latitudes for different depths. The TW leaves the boundary between 35.4S and 36.5S while the NADW is still

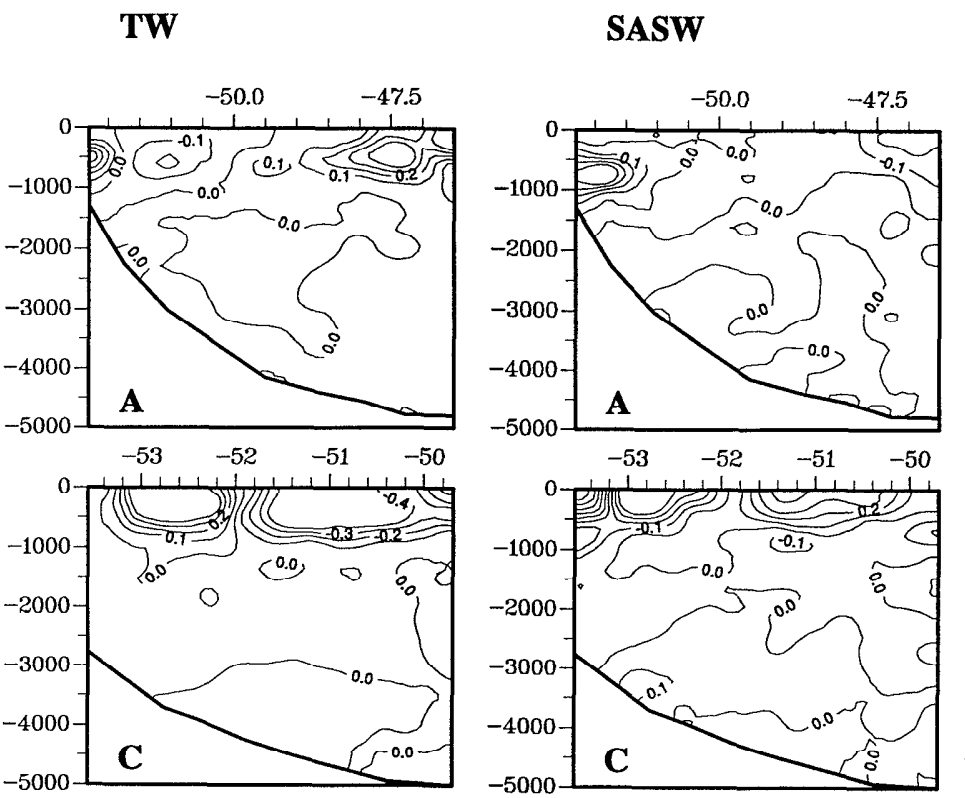

Figure 6. Difference between the proportions of each source water type during Confluence 1 and Confluence 2 along sections A and C: (a) Thermocline Water (TW) and Subantarctic Surface Water (SASW), (b) Antarctic Intermediate Water (AAIW) and Upper Circumpolar Deep Water (UCDW), (c) North Atlantic Deep Water (NADW) and Lower Circumpolar Deep Water (LCDW).

observed on the continental slope at 36.5S. The large volume occupied by AAIW in the north during winter (Maamaatuaiahutapu *et al.*, 1992) is also obtained during spring. This is supported by the fact that the northern component of the AAIW locally recirculates in an anticyclonic cell as suggested by Reid *et al.* (1977).

To proceed further in the comparison between the two data sets, we compute the SWT proportions obtained in spring minus those calculated in the winter season. Figure 6 shows this difference between the proportions of each SWT during Confluence 1 (spring 1988) and Confluence 2 (winter 1989). Table 2 reports the percentage of water samples with standard deviation lower than the 5%, 10% and 15% criteria for the two cruises. For the SWT difference, these criteria would be multiplied by a factor of 2. Thus, the absolute values of the SWT differences higher than 30%, are significant for all samples. The 10% and 20% criteria are valid for 90% and 95% of the total number of samples, respectively. Sections A and C are retained

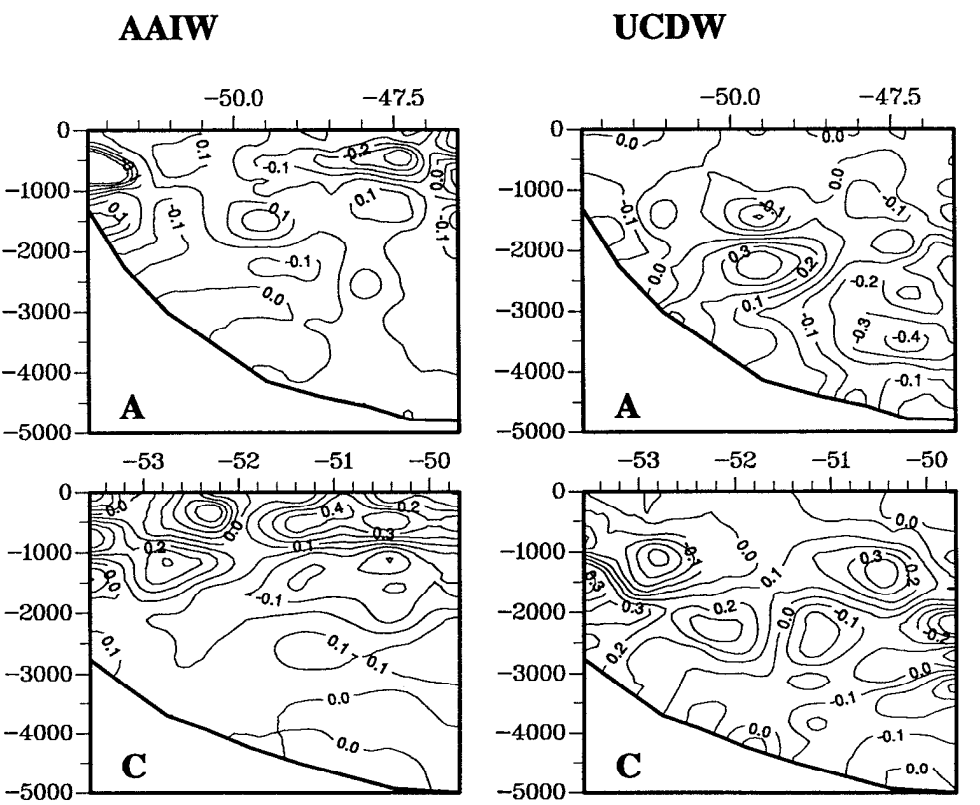

Figure 6. (Continued)

for the comparison whereas section B is omitted since only three out of the six CTD stations common to both cruises extend to the bottom. In the following discussion, the results from each of the Confluence cruises are referred to by their season; that is we use the term "spring" for the Confluence 1 cruise period and "winter" for the Confluence 2 cruise period.

The surface waters undergo significant changes between the Confluence 1 and Confluence 2 cruises. This is not surprising as they are under direct atmospheric influence. At 35.4S east of 48W, the subtropical waters of the Brazil Current are present in higher proportions in spring than in winter. At 37.9S, they are observed (west) east of 52W in (lower) higher percentage during winter than during spring. The subantarctic waters of the Malvinas Current are found west of 51W at 35.4S in larger quantities during spring than during winter. At 37.9S, their presence west (east) of 52W is increased (reduced) during winter. The seasonal change in spatial distribution of water mass contributions for the upper layers is related to the fluctuations in time and space of the thermohaline front. The front during the spring of 1988 has a north-south orientation. Excursion of the cold water tongue associated

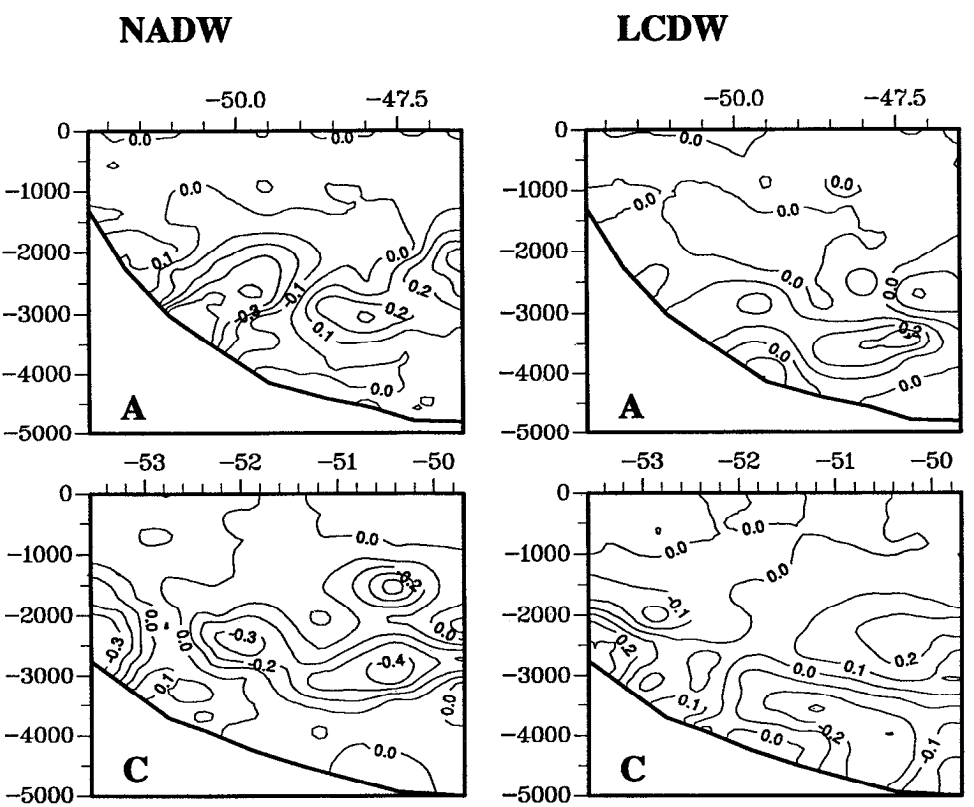

Figure 6. (Continued)

with the Malvinas Current is visible on section A parallel to the edge of the continental shelf. During the winter of 1989, the front axis is tilted, the orientation being north-northwest south-southeast. The northern boundary of the Malvinas Current (between 35.4S and 36.5S) is located farther south compared with the preceding spring. The transition zone between the subtropical boundary current extension and the subantarctic front, i.e. the Malvinas, is wider during this winter month. The shape of the southern limit of the Brazil Current is also distinct during each cruise. The Brazil Current separation from the shelf break is seen here farther north at mid-winter (September) than it is in the spring (November).

Motions of the front have been examined through satellite Sea Surface Temperature (SST) data (Olson *et al.,* 1988; Garzoli *et al.,* 1992). With synoptic SST fields, Olson *et al.* (1988) and Garzoli *et al.* (1992) try to locate the frontal position during different seasons. This is difficult to perform with sparse hydrographic data. However, at 38S, with eight repeated vertical sections, we can define the longitudinal position of the front at different periods. Figure 7 reports the longitudinal position of the western wall based on the 8°C isotherm of the Brazil Current at 38S for various

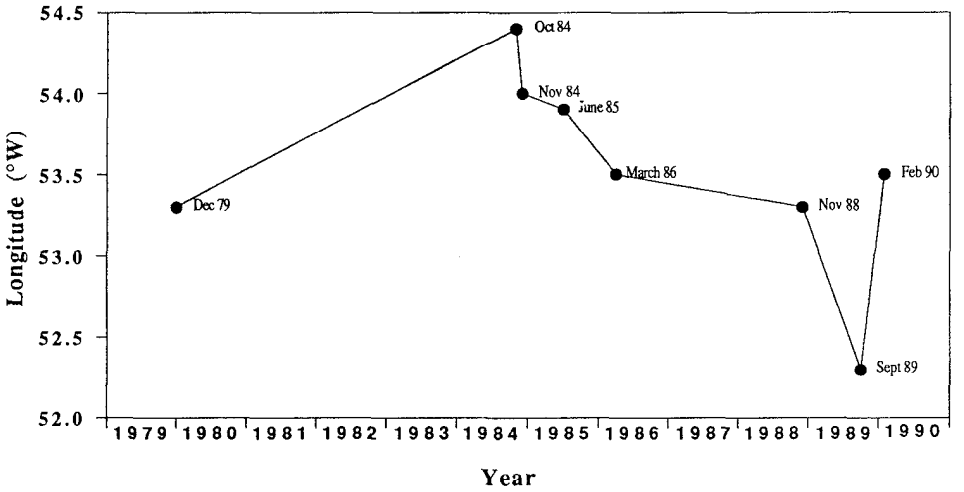

Figure 7. Longitudinal location of the west wall of the Brazil Current around 38S from various oceanographic cruises: December 1979 (Gordon, 1981), October 1984 (Gordon, 1989), November 1984 and June 1985 (Garzoli and Bianchi, 1987), March 1986 (Garzoli and Garraffo, 1989), November 1988 and September 1989 (Charo *et al.*, 1991), February 1990 (Provost *et al.*, 1991).

oceanographic cruises. The values fluctuate around a mean value of 53.6S. The largest departures from the mean is 100 km (54.5W) to the west and 144 km (52.3W) to the east. The largest variation in the longitudinal position of the Brazil Current wall is between the two winter seasons 1984 and 1989. At 38S, the front exhibits both interannual and annual cycles but can be perturbed on shorter time scales (Provost *et al.*, 1992) in relation with sporadic intrusion of the Malvinas current to the north (Garzoli and Garraffo, 1989). With Geosat altimeter data, Matano *et al.* (1992) show that the latitude of the confluence between the Brazil and Malvinas Currents is located farther north during winter than summer. However, between the spring and the winter seasons, their Figure 6 shows that the confluence may be positioned further north in spring as well as in winter.

One interesting feature to note is that the pronounced percentage differences between the solutions obtained during the two cruises occur at the same longitudes for the warm Brazil, cold Malvinas and Antarctic Intermediate waters (Fig. 6). On the northernmost section A, this coincidence is found only for the Thermocline and Antarctic Intermediate waters. A larger amount of AAIW is observed in winter than in spring on the 35.4S section. On section C, the reverse is seen, with lower proportions of AAIW in winter than in spring. Within the confluence region, the spreading path of the AAIW is largely influenced by the positioning of the two strong surface currents. Nevertheless, the two Confluence 1 and 2 cruises are separated by a 9-month period (summer and fall of 1989) and little can be ascertained concerning a probable route for AAIW during this time lag given current data resources.

Traditionally, the western boundary of the southwestern Atlantic Ocean is viewed as a layered current system with warm tropical water flowing southward over northward AAIW which lies above the southward flowing NADW. Some investigators showed that the northward flow of AAIW does not take place everywhere along the western boundary but only south of about 40S in the Malvinas Current and north of about 25S (Reid *et al.,* 1977; Evans and Signorini, 1985; Reid, 1989). Between those latitudes, the AAIW flows eastward as part of the subtropical gyre; south of 20S, when the westward-flowing northern limb of the gyre approaches the coast of South America, a part is continuing southward around the gyre and the other one is continuing northward (Reid, 1989; Warner and Weiss, 1992). Reid (1989) however concludes that the matter of a narrow northward boundary current west of the gyre was not really resolved. No narrow northward flowing branch of AAIW (the possible existence of which is mentioned by Reid (1989)) is observed in the Confluence data sets. Recently, Gordon *et al.* (1992) suggest that rather than follow a route along the western boundary of the South Atlantic, thc bulk of AAIW may first flow across the South Atlantic and through the southwest Indian ocean before spreading northward in the subtropical South Atlantic Ocean. During the two Confluence cruises, the persistent feature of a larger amount of AAIW on the northern sections (in the latitude range 35.4–37.9S) than on the southernmost sections (39–41.6S) confirms a southward route of AAIW. Maamatuaiahutapu (1993), studying the circulation in the Confluence area with a nonlinear inverse model, shows that, along the northern boundary of the investigated area, the AAIW flows southward. Similarly, this southward travel of the intermediate waters has been demonstrated in a high resolution global ocean general circulation model (England and Garçon, 1994). This flow régime exists in both the Reid (1989) and Gordon *et al.* (1992) schemes.

The difference in SWT proportions between Confluence 1 and 2 data sets displays large spatial variation at the level of the deep waters (Fig. 6). Common spatial occurrence of NADW at the 2500 m level during the two cruises is rare. The NADW is found in greater (lower) amount west (east) of 49.5W during winter than during spring on section A. The NADW core on the east of section A during spring would indicate that the NADW had left the continental slope at a lower latitude than during the winter. This is confirmed by the strong presence farther south on section C during winter. The NADW winter contribution to the water samples is predominant along the whole of section C.

The UCDW is less perturbed by the upper layer than by the NADW on section A (Fig. 6). The main difference in spring and winter proportions of the UCDW on section A occurs in the 1500–2500 m range. The UCDW is wedged in between the NADW and the continental slope during spring while during winter, it is displaced eastward by NADW. For depths shallower than 1500 m, the UCDW is as present in winter as it is during spring. On section C, the UCDW is influenced by the relative position of AAIW and NADW. Isolated patches of UCDW seem to be present at the

same longitudes in winter and spring, except at 52W where it is visible only in springtime.

The LCDW proportions during the two cruises show some minor differences. On section C, the LCDW location is dependent upon the NADW distribution during the two seasons. The variation of proportions of the abyssal WSDW between the two seasons in the Argentine Basin is not significant.

Except at the lowest level of the WSDW, the deep waters are submitted to considerable variation in their location during spring and winter. This variation largely depends upon the position of the convergence between the northern and southern waters as it occurs at the sea surface. The NADW is more concentrated farther south during the winter cruise than during the spring cruise suggesting a stronger southward deep current in winter than in spring. The CDW follows a reverse scheme and its northward excursion is governed by the presence of NADW in the area. The eastward movement of CDW occurs at different latitudes for the different cruises. Comparison with previous data sets of the NADW southward excursion can be made on the basis of a high salinity core representing NADW. The comparison can only be carried out on the 38S section. Two vertical salinity sections are reported at two different seasons, spring 1979 by Gordon (1981) and winter 1984 by Gordon (1989). If we consider the 34.9 psu salinity core, the NADW occupies a larger volume during spring 1979 than during winter 1984 on the continental slope. During the Confluence cruises, we observe a reverse situation. The southward extension of NADW seems related to the position of the surface front. The NADW concentration is less intense at 38S when the NADW is located beneath the TW than when found below the SASW. This intercomparison between both Confluence and Gordon (1981, 1989) sections shows that the deep variations are more likely to be longer time scale variability than seasonal variability.

7. Summary

The multiparameter computation is efficient in the SWT analysis in gathering the information brought out by multiple tracers. The application to the new Confluence 1 data set confirms the large-scale circulation aspects inferred previously from the Confluence 2 data set (Maamaatuaiahutapu *et al.,* 1992).

The multiparameter analysis enables a quantitative comparison between SWT proportions of the two data sets, documenting for the first time the SWT proportions variations at two different seasons. The Confluence data show that the positions of the surface waters strongly depend upon the location of the Brazil/Malvinas front. The intrusion of SASW is located farther north in the region during winter 1989 than during spring 1988. The influence of the movement of the surface front seems reflected through AAIW down to the level of NADW. The AAIW spatial distribution varies when the TW and SASW have changed in location. The deep water

variations between the two cruises are evidenced in the poleward extension of the NADW and the northward intrusion of CDW along the western boundary.

Acknowledgments. We acknowledge the dedicated efforts of the officers and crew of the two Argentine research vessels *Puerto Deseado* and *Oca Balda.* Comments by M. H. England, J. F. Minster and two anonymous reviewers are greatly appreciated. The project was funded by a grant of the Centre National de la Recherche Scientifique (PNEDC: WOCE, CO_2) to UMR39 and LODYC.

REFERENCES

Boulahdid, M. 1987. Analyse des sels nutritifs dans l'eau de mer. Etude du mélange des masses d'eau et de l'oxydation de la matière organique dans l'océan. Thèse de Doctorat, Univ. Paris VII, 266 pp.

Charo, M., A. P. Osiroff, A. Bianchi and A. R. Piola. 1991. Datos fisico-chimicos, CTD y XBT, Campañas oceanograficas Puerto Deseado 02-88, Confluencia 88 y Confluencia 89. Inf. Tec. 59/1991, Buenos Aires, Serv. de Hidrogr. Nav., 422 pp.

Confluence Group. 1990. Confluence 1988–1990: An intensive study of the southwestern Atlantic. EOS Trans. Amer. Geophys. Un., *71,* 1131–1134.

England, M. H. and V. C. Garcon. 1994. South Atlantic circulation in a World Ocean model. Annales Geophysicæ, Special Edition on the South Atlantic Ocean, in press.

Evans, D. L. and S. S. Signorini. 1985. Vertical Structure of the Brazil Current. Nature, *315,* 48–50.

Garçon, V. C., M. Boulahdid, K. Maamaatuaiahutapu and B-Y Boudjellal. 1991. Rapport des campagnes à la mer Confluence-1, novembre 1988; Confluence-2, septembre 1989; Confluence-3, février 1990: Données de sels nutritifs. Rapp. interne UMR 39/GRGS 91.103., Groupe de Recherche de Géodésie Spatiale, Toulouse, 207 pp.

Garzoli, S. L. and A. Bianchi. 1987. Time-space variability of the local dynamics of the Malvinas-Brazil Confluence as revealed by inverted echo sounders. J. Geophys. Res., *92,* 1914–1922.

Garzoli, S. L. and Z. Garraffo. 1989. Transports, frontal motions and eddies at the Brazil-Malvinas currents confluence. Deep-Sea Res., *36,* 681–703.

Garzoli, S. L., Z. Garraffo, G. Podesta and O. Brown. 1992. Analysis of a general circulation model product, 1, frontal systems in the Brazil/Malvinas and Kuroshio/Oyashio regions. J. Geophys. Res., *9,* 20,117–20,138.

Georgi, D. T. 1981a. On the relationship between the large-scale property variations and fine structure in the circumpolar deep water. J. Geophys. Res., *86,* 6556–6566.

—— 1981b. Circulation of bottom waters in the Southwestern South Atlantic. Deep-Sea Res., Part A, *28,* 959–979.

Gordon, A. L. 1981. South Atlantic thermocline ventilation. Deep-Sea Res., *28,* 1239–1264.

—— 1989. Brazil-Malvinas confluence—1984. Deep-Sea Res., *36,* 359–384.

Gordon, A. L., R. F. Weiss, W. M. Smethie, Jr., and M. J. Warner. 1992. Thermocline and Intermediate Water communication between the South Atlantic and Indian oceans. J. Geophys. Res., *97,* 7223–7240.

Greengrove, C. L. 1986. Thermohaline Alteration of the South Atlantic Pycnocline. Ph.D thesis, Columbia University, New York, 211 pp.

Lawson, C. L. and R. J. Hanson. 1974. Solving Least Squares Problems. Prentice-Hall, Englewood Cliffs, New Jersey, 340 pp.

Legeckis, R. and A. L. Gordon. 1982. Satellite observations of the B azil and Falkland currents—1975 to 1976 and 1978. Deep-Sea Res., *29,* 375–401.

Maamaatuaiahutapu K. 1993. Etude de la circulation dans la région de Confluence des courants du Brésil et des Malouines. These de doctorat de l'Université Paul Sabatier (Toulouse), 368 pp.

Maamaatuaiahutapu, K., V. C. Garcon, C. Provost, M. Boulahdid and A. P. Osiroff. 1992. Brazil-Malvinas Confluence: water mass composition. J. Geophys. Res., *97,* 9493–9505.

Mackas, D. L., K. L. Denman and A. F. Bennett. 1987. Least squares multiple tracer analysis of water mass composition. J. Geophys. Res., *92,* 2907–2918.

Matano, R. P., M. G. Schlax and D. B. Chelton. 1992. Seasonal variability in the Southwestern Atlantic. J. Geophys. Res., *98,* 18,027–18,035.

Menke, W. 1989. Geophysical Data Analysis: Discrete Inverse Theory. Int. Geophys. Ser., Academic Press, San Diego, Calif., *45,* 289 pp.

Olson, D. B., G. P. Podestá, R. H. Evans and O. B. Brown. 1988. Temporal variations in the separation of Brazil and Malvinas currents. Deep-Sea Res., *35,* 1971–1990.

Peterson, R. G. 1992. The boundary currents in the western Argentine basin. Deep-Sea Res., *39,* 623–644.

Peterson, R. G. and L. Stramma. 1991. Upper-level circulation in the south Atlantic Ocean. Prog. Oceanogr., *23,* 149–244.

Peterson, R. G. and T. Whitworth. 1989. The subantarctic and polar fronts in relation to deep water masses through the southwestern Atlantic. J. Geophys. Res., *98,* 10,817–10,838.

Provost, C., O. Garcia and V. Garçon. 1992. Analysis of satellite sea surface temperature time series in the Brazil-Malvinas current confluence region: Dominance of the annual and the semiannual periods. J. Geophys. Res., *97,* 17,841–17,858.

Provost, C., L. Mémery and B. Torres Lista. 1991. Confluence 3: Données CTD-O2, Rapp. Interne LODYC 91/02, 188 pp., Lab. d'Océanogr. Dyn. et de Climatol., Paris.

Reid, J. L. 1989. On the total geostrophic circulation of the South Atlantic Ocean: Flow patterns, tracers, and transports. Prog. Oceanogr., *23,* 149–244.

Reid, J. L., W. D. Nowlin Jr. and W. C. Patzert. 1977. On the characteristics and circulation of the southwestern Atlantic Ocean. J. Phys. Oceanogr., *7,* 62–91.

Takahashi, T., J. Goddard, D. W. Chipman and M. Noonan. 1990. Carbon chemistry in the confluence areas of the Brazil and Malvinas currents in the southwestern Atlantic Ocean: The results of the Confluence-89 expedition in September, 1989. Technical report, Lamont-Doherty Geol. Observ., Columbia Univ., Palisades, New York, 38 pp.

Tomczak, M. 1981. A multi-parameter extension of temperature/salinity diagram techniques for the analysis of nonisopycnal mixing. Progr. Oceanogr., *10,* 147–171.

Warner, M. J. and R. F. Weiss. 1992. Chlorofluoromethanes in South Atlantic Antarctic Intermediate Water. Deep sea Res., *39,* 2035–2075.

Received: *30 March, 1993;* revised: *9 December, 1993.*